Time evolution of dynamic shear moduli in a physical gelation process of 1,3:2,4-bis-O-(*p*-methylbenzylidene)-D-sorbitol in polystyrene melt: Critical exponent and gel strength

Mikihito Takenaka,[1] Toshiaki Kobayashi,[1,*] Takeji Hashimoto,[1,†] and Masaoki Takahashi[2]
[1]*Department of Polymer Chemistry, Graduate School of Engineering, Kyoto University, Kyoto 606-8501, Japan*
[2]*Department of Polymer Science and Engineering, Kyoto Institute of Technology, Matsugasaki, Kyoto 606-8585, Japan*
(Received 27 April 2001; revised manuscript received 3 December 2001; published 1 April 2002)

We investigated time evolution of shear moduli in the physical gelation process of 1,3:2,4-bis-O-(*p*-methylbenzylidene)-D-sorbitol (PDTS) in the polystyrene melt system containing 2.5 wt % of PDTS. At the gel point, storage and loss shear moduli, G' and G'', were described by the power law of frequency ω, $G' \sim G'' \sim \omega^n$, with the critical exponent n equal to $\frac{2}{3}$, in agreement with the value predicted by the percolation theory. The exponent n and the gel strength S at the gel point measured as a function of quench depth ΔT indicated that the fractal network structure of PDTS does not change with ΔT but that the mechanical strength of the network increases with ΔT. Before reaching the gel point, $G'(\omega)$ and $G''(\omega)$ obtained at various times can be well superposed onto the master curves, indicating that the mechanical as well as structural self-similarity hold in this gelation process.

DOI: 10.1103/PhysRevE.65.041401 PACS number(s): 82.70.Gg, 83.80.Kn, 83.60.Bc

I. INTRODUCTION

1,3:2,4-bis-O-(*p*-methylbenzylidene)-D-sorbitol (PDTS) has such a remarkable property that a small amount of it, by less than 10 wt %, forms gels in organic solvents and polymer melts [1]. This property of PDTS as a gelation agent has been used in the processing of a paste sol (homogeneous solution) of polyvinylchloride (PVC) and dialkyl (C4-12) phthalates (DAP) as a plasticizer (designated hereafter PVC/DAP) [2]. The gelation of PDTS in PVC/DAP with a small amount of PDTS (designated hereafter PVC/DAP/PDTS) modifies the viscoelastic properties of the system so that its paste can easily be processed. It has been found that the formation of the gel networks is caused by the crystallization or solid-liquid phase transition of the supersaturated PDTS into a percolated network in the solution of PVC/DAP/PDTS. The sol-gel transition of PDTS solution in the system is thermoreversible, and the transition temperature decreases with increasing solubility of PDTS to its solvent or matrix of PVC/DAP. Formation of the percolated network of PDTS with a large specific surface area in the molten crystallizable polymers may act as a heterogeneous nucleus and hence, enhance the nucleation rate of the polymers, when a small amount of PDTS is mixed with crystallizable polymers. The enhancement may create a large number of small crystalline superstructures, resulting in increased transparency of the crystallized polymers. Moreover, we may control the mechanical properties of the crystallized polymers as well, while keeping their optical clarity, by controlling the network structures of PDTS. Thus, it is important to explore the mechanism of the sol-gel transition process of PDTS systems. In this paper, we investigated this mechanism by means of rheological measurements.

The viscoelastic behaviors of polymer gels near the sol-gel transition have been studied experimentally [3–13] and theoretically [14–19]. Experimental studies reported that the percolation theory can be quite successful in describing the viscoelastic properties near the sol-gel transition. However, until now most of the experimental studies have been done for chemical gels and only a few experiments for physical gels. In particular, the viscoelastic behaviors of physical gels near sol-gel transitions have not been well studied yet and thus, the mechanism of its sol-gel transition has not been completely clarified. In this paper, we explored PDTS in a polystyrene (PS) melt (hereafter defined as PDTS/PS) as a typical model system for physical gelation process and investigated a time evolution of dynamic viscoelastic behavior of the system after a temperature quench below the gel point. The objectives of the present study are as follows.

(i) To clarify the differences or similarities in viscoelastic behaviors in the physical gelation process of the PDTS system compared with those in a chemical gelation process.

(ii) To obtain the critical exponent and the gel strength when there are scaling relationships in the gelation process as general critical phenomena.

II. THEORETICAL BACKGROUND

When networks grow, either via physical or chemical gelation process, with self-similarity before reaching the sol-gel transition point, the networks are characterized by an upper cutoff length of the clusters of the networks, ξ, and the fractal dimension d_f [14,15] of the networks. ξ can be described by

$$\xi \sim \varepsilon^{-\nu}, \tag{1}$$

where ε and ν are, respectively, the relative distance of a point of observation in the sol state from the gel point and the critical exponent. The distance ε is given by

*Present address: Research and Development Division, New Japan Chemical Co., 13 Yoshijima, Yagura-Cho, Fushimi-Ku, Kyoto 615-8224, Japan.
†Author to whom correspondence should be addressed.

$$\varepsilon = |p - p_c|/p_c, \tag{2}$$

where p and p_c are the extents of a ''reaction'' before the gel point and at the gel point, respectively. In our experiment, the extent of the reaction corresponds to the crystallinity of the PDTS induced by the solid-liquid transition. Before the gelation point, the zero-shear viscosity η_0, steady state compliance J_e^0, and the terminal relaxation time τ scale as

$$\eta_0 \sim \varepsilon^{-k}, \tag{3}$$

$$J_e^0 \sim \varepsilon^{-z}, \tag{4}$$

and

$$\tau \sim \eta_0 J_e^0 \sim \varepsilon^{-(k+z)}. \tag{5}$$

In polymer systems where hydrodynamic interactions are completely screened out (corresponding to Rouse limit) and the excluded volume effects are dominant, the critical exponents k and z are given by [14,15]

$$k = \nu(d_f + 2 - d), \tag{6}$$

$$z = \nu d \tag{7}$$

with d_f and d (equal to 3 in our case) being the fractal dimension and space dimensionality, respectively. On the other hand, if excluded volume effects as well as hydrodynamic interactions are completely screened out, k is expressed by

$$k = \nu(\bar{d}_f + 2 - d), \tag{8}$$

with

$$\bar{d}_f = \frac{2d_f}{d + 2 - 2d_f}, \tag{9}$$

while z has the same form as Eq. (7).

Theoretically, Martin, Adolf, and Wilcoxon predicted $k = 1.33$ and $z = 2.67$ using $\nu = \frac{8}{9}$ and $d_f = 2.5$ for three-dimensional space with $d = 3$ [14]. Takigawa *et al.* derived a different value of z, $z = 2.28$, in terms of the equilibrium modulus G_{eq} after the gelation point by considering the fractal dimensions for minimum path and backbone in networks [19]. The values of k and z are also predicted from the analogy between gelation and electrical networks. de Gennes showed that the equilibrium modulus of a gel should correspond to the conductivity in a random resistor-insulator network [20]. Computer simulation based on this analogy gives $z = 1.94 \pm 0.10$ [21]. In these treatments the effect of the ''blobs'' [13] on the modulus of critical gel is ignored, and dangling chains are assumed not to contribute to the modulus. de Gennes also proposed an analogy between the divergence of viscosity and the divergence in the conductivity in a random superconductor-resistor network [22]. Simulation of superconductivity gives $k = 0.75 \pm 0.04$ [23]. Experimentally, Takahashi, Yokoyama, and Masuda found $z = 2.0$–2.1 for G_{eq} while $z = 2.7$–2.8 for J_e^0 [13] in an end-linking polymer system. They suggested that this discrepancy is due to the following fact: links in the backbone structure determine the critical exponent for G_{eq} while the blobs and dangling chains besides the links incorporated into the network were considered to contribute J_e^0.

Self-similarity in the cluster growth at a given ε is expected to give the mechanical self-similarity [11–13] as well. This self-similarity makes it possible to superpose angular frequency dependence of G' and G'' obtained at different p's ($p < p_c$) to give universal curves $G' a_v$ vs ωa_h and $G'' a_v$ vs ωa_h, where a_v and a_h are, respectively, vertical and horizontal shift factors at each p in the double logarithmic plot of $\log_{10} G'$ and $\log_{10} \omega$. The shift factors a_v and a_h are defined by

$$a_v = \frac{J_e^0(p)}{J_e^0(p_r)} = \left[\frac{\varepsilon(p)}{\varepsilon(p_r)}\right]^{-z} \tag{10}$$

and

$$a_h = \frac{\tau(p)}{\tau(p_r)} = \left[\frac{\varepsilon(p)}{\varepsilon(p_r)}\right]^{-(k+z)}, \tag{11}$$

where $\varepsilon(p_r)$ is the value ε at a given reference reaction extent p_r. From Eqs. (10) and (11), we can obtain

$$\frac{\log_{10} a_v}{\log_{10} a_h} = \frac{z}{k+z}, \tag{12}$$

indicating that $\log_{10} G'(\omega)$ and $\log_{10} G''(\omega)$ at different p's ($p < p_c$) plotted as a function of $\log_{10} \omega$ can be superposed on each other by shifting along a straight line with the slope of $z/(k+z)$.

At gel point ($p = p_c$), stress relaxation moduli $G(t)$, G', and G'' show the following power-law behavior [3]:

$$G(t) = St^{-n}, \tag{13}$$

and

$$G' \sim G'' \sim \omega^n, \tag{14}$$

where gel strength S characterizes the strength of the gel at gel point. It should be noted that the power-law behavior is limited to a finite frequency range due to the characteristic time of building block of the gel. Moreover, the power-law behavior for physical gels should be more limited than that for chemical gels because of a finite lifetime of the physical bonds [3]. According to the theory of linear viscoelasticity [24],

$$G'(\omega) = \omega \int_0^\infty G(t) \sin(\omega t) dt. \tag{15}$$

Substituting Eq. (13) into Eq. (15) we can obtain

$$S = \frac{2\Gamma(n)\sin(n\pi/2) G'(\omega)}{\pi \omega^n}, \tag{16}$$

where $\Gamma(n)$ is the gamma function.

The power law is predicted by Martin, Adolf, and Wilcoxon [14], Rubinstein, Colby, and Gillmor [15], Muthukumar [16,17], and Hess, Vilgis, and Winter [18]. It postulates that the longest relaxation time of the gel diverges with the

same critical exponent from both sides of the gel point, a general expression for n is given by

$$n=\frac{z}{k+z}. \tag{17}$$

When hydrodynamic interactions are completely screened out and the excluded volume effects are dominant in the cluster, we obtain

$$n=\frac{d}{d_f+2} \tag{18}$$

from Eqs. (6), (7), and (17). On the other hand, if excluded volume effects as well as hydrodynamic interactions can be completely screened out, n is expressed by

$$n=\frac{d(d+2-2d_f)}{2(d+2-d_f)} \tag{19}$$

from Eqs. (7)–(9) and (17) [17]. If the power law of Eq. (14) holds over a sufficiently wide range of ω at gel point, the loss tangent, $\tan\delta$, at gel point is given by

$$\tan\delta=\tan\left(\frac{n\pi}{2}\right) \tag{20}$$

from the Kramers-Kronig relation [24], indicating that $\tan\delta$ is independent of ω at gel point and its value depends only on n.

III. EXPERIMENTAL SECTION

A. Samples

The synthesis of PDTS was described in detail elsewhere [25]. In this work we explored physical gelation of PDTS/PS. The weight-averaged molecular weight, Mw, and heterogeneity index, Mw/Mn, of PS are, respectively, 6.4×10^4 and 1.03, where Mn is the number-average molecular weight. The concentration of PDTS in PDTS/PS is 2.5 wt. %. PDTS/PS was first dissolved into a dioxane solution at 60 °C to prepare a homogeneous solution containing 10 wt % of PDTS/PS. The solution was then frozen at −60 °C for 40 min and dried for 40 h in a vacuum in order to obtain the frozen homogeneous mixture of PDTS/PS free from dioxane. We molded the freeze-dried sample at 200 °C and 150 Kg/cm^2 into a disk 2 mm thick and 25 mm in diameter, and the disk was then rapidly quenched into cold water. The as-prepared disk, which is a vitrified homogeneous mixture of PDTS/PS was used for further experiments. We also prepared PS samples without PDTS in the same manner and used them as reference materials for the PDTS/PS samples.

B. Viscoelastic measurements

Dynamic viscoelastic measurements have been made during the gelation process using the Rheometrics Mechanical Spectrometer®. We set the disk sample of PDTS/PS into parallel plates of 25 mm diameter and annealed at 220 °C for 2 min to make the sample in sol state. Subsequently, we quenched the sample to 183, 181, and 173 °C, where the system undergoes the sol-gel transition. Note that the sol-gel transition temperature was determined to be (180±2) °C in the cooling process [26]. Then we measured frequency dependencies of storage and loss moduli, G' and G'', every 5 min at each frequency in the frequency range from 0.1 to 100 s^{-1}. The strain was 0.1 in the linear viscoelastic criterion. We also measured the frequency dependencies of G' and G'' for PS in the frequency range from 0.1 to 100 s^{-1} at 183, 181, and 173 °C.

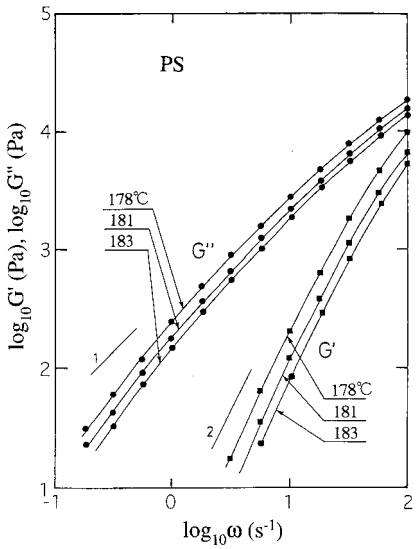

FIG. 1. Frequency dependence of G' and G'' of PS at 183, 181, and 178 °C.

IV. RESULTS AND DISCUSSION

A. Viscoelasticity of PS

Figure 1 shows the frequency dependencies of G' and G'' of PS at 178, 181, and 183 °C. G' and G'' measured as a function of ω at each temperature follow the power law of $G'\sim\omega^1$ and $G''\sim\omega^2$ at low frequencies, manifesting itself, the PS melt being a viscoelastic liquid of flow region in the observed ω range at the measured temperatures. The critical entanglement molecular weight of PS is $\sim3.5\times10^4$ so that the PS used in this study is slightly entangled, though the rubbery region is not observed in the measured ω region. These data were used for the analysis of the gelation process as will be discussed in the following sections.

B. Change in viscoelasticity during gelation process with time

Figures 2 and 3 show changes in G' and G'' with time at fixed ω's after the onset of the gelation at 183 °C. G' and G'' increase with time at all observed ω region, indicating that the PDTS aggregates and forms clusters of networks in PS matrix and that the amount and size of the clusters of the networks formed increase with time. The measured G' and G'' values for PDTS/PS include not only the contribution of the PDTS clusters but also that of PS matrix. Thus, we assume the measured G' and G'' values for PDTS/PS are a

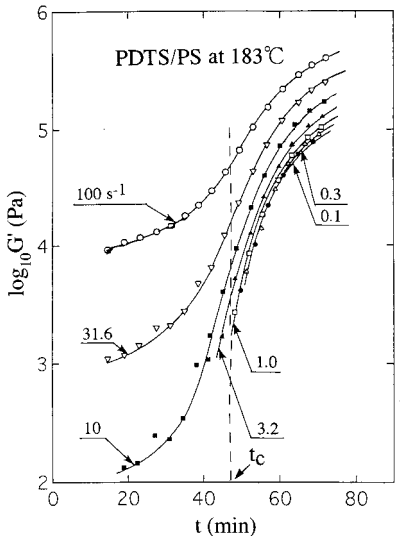

FIG. 2. Changes in G' at fixed ω's with t during the gelation process of the PDTS/PS system at 183 °C. t_c is the gel point assessed from Fig. 4.

sum of those from PDTS clusters and those from PS matrix. In these figures, the G' and G'' values are due to those effective for the PDTS clusters, which were obtained by subtracting the G' and G'' values of pure PS melt (shown in Fig. 1) from net values of G' and G'' of PDTS/PS, for further analysis of the gelation process. The vertical dashed line indicates the gel point t_c as will be discussed later.

C. Change in tan δ

Figure 4 shows changes in tan δ with time at fixed ω's after the quench to 183 °C. From the time change in tan δ, the gelation process can be divided into the following three

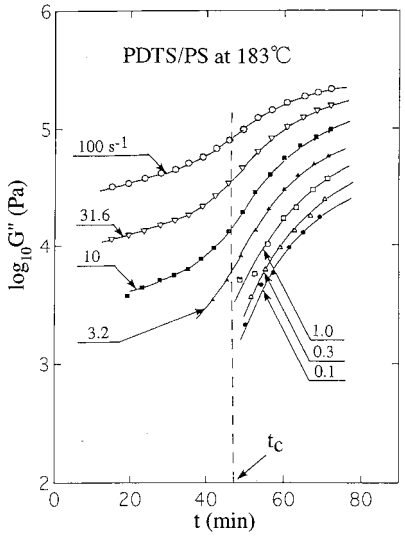

FIG. 3. Changes in G'' at fixed ω's with t during the gelation process of the PDTS/PS system at 183 °C. t_c is the gel point assessed from Fig. 4.

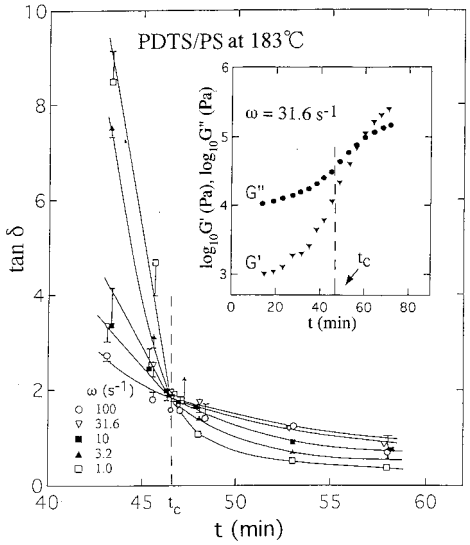

FIG. 4. Change in tan δ at fixed ω's during the gelation process of the PDTS/PS system at 183 °C. Inset displays the changes in G' and G'' at $\omega = 31.6\ \mathrm{s}^{-1}$ with t, where the vertical dashed lines indicate the gelation point ($t_c = 46.8$ min) at 183 °C.

stages with respect to a characteristic time t_c for formation of the critical gel (t_c being 46.8 min at 183 °C as will be detailed below).

(i) At $t < t_c$, G' increases more rapidly than G'', and thus tan δ decreases rapidly with t. The tan δ value is larger at lower ω's. In this region, PDTS forms the networks that are not macroscopically percolated yet: The clusters of the networks have the upper cutoff size ξ.

(ii) At $t = t_c$ tan δ becomes independent of ω. This indicates that the system has reached the gel point and that the clusters of the networks with macroscopically percolated or with infinitely large molecular weight is formed.

(iii) At $t > t_c$ the clusters are linked into three-dimensionally interconnected networks. G' still increases faster than G'' but its growth rate becomes moderate. As a result tan δ decreases gradually with t.

The inset of Fig. 4 shows the time changes in G' and G'' at $\omega = 31.6$ rad/s. It should be noted that G'' is larger than G' at the gel point indicated by an arrow.

Figure 5 shows changes in tan δ with time in the case of the quench to lower temperatures (181 and 178 °C). The behaviors similar to those at 183 °C were observed in the curves of tan δ vs t, except for the fact that t_c decreases with decreasing temperature. We can calculate the values of n from tan δ at t_c by using Eq. (20). The values of t_c, tan δ at gel point, and the exponent n, $n_{\tan}$, obtained from the tan δ at gel point at each gelation temperature are summarized in Table I. The strength S of the gel calculated using Eq. (16) is also listed in Table I. The temperature dependence of n and S will be discussed later.

D. Viscoelasticity at the gel point

Figure 6 shows the frequency dependences of G' and G'' at the gel point (defined, respectively, by G'_c and G''_c) at each

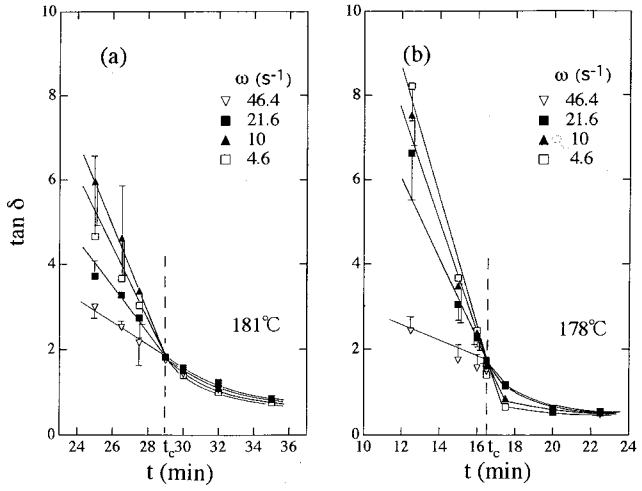

FIG. 5. Change in tan δ at fixed ω's during the gelation process of the PDTS/PS system at 178 °C (a) and 181 °C (b).

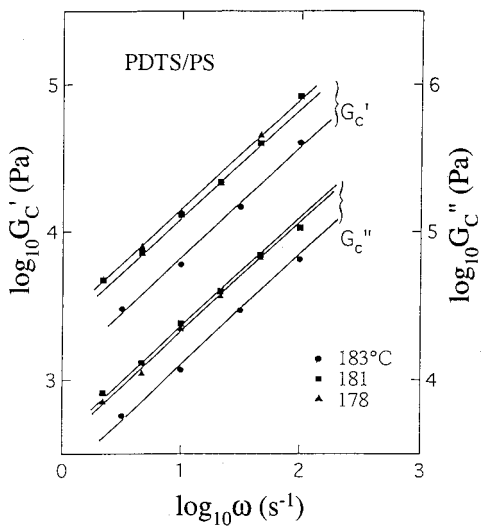

FIG. 6. Shear moduli G'_c and G''_c at gel point plotted as a function of ω in double logarithmic scale for the gelation of the PDTS/PS system at 183, 181, and 178 °C. Solid lines indicate the best-fitting results with the power-law behavior with $n=n_{\mathrm{slope}}$ in Table I [Eq. (14)].

gelation temperature. In order to obtain $G'_c(\omega)$ and $G''_c(\omega)$ at each gelation temperature, we interpolated the values $G'(\omega)$ and $G''(\omega)$ at t_c from the curves of $G'(\omega)$ vs t and $G''(\omega)$ vs t at each temperature as shown in Figs. 2 and 3, respectively. It should be noted here that G'_c and G''_c in Fig. 6 were corrected for those for the pure PS melt shown in Fig. 1. The plots of $\log_{10} G'_c(\omega)$ and $\log_{10} G''_c(\omega)$ vs $\log_{10}\omega$ at each temperature become linear and parallel to each other. Thus G' and G'' obey the power law of ω as described by Eq. (14). We estimated the values n, n_{slope} from the plots of $\log_{10} G'$ and $\log_{10} G''$ vs $\log_{10}\omega$, at each gelation temperature and listed them in Table I. The values of n_{slope} agree with those of $n_{\tan}$, indicating that the experimental results confirm theoretical consistency as described in Sec. II. The values of n thus estimated are almost independent of temperature and agrees with the value of $\frac{2}{3}$ predicted by the percolation theory of Eq. (18) with $d_f=2.5$ [14].

While n is independent of the quench depth, S increases with decreasing temperature. This fact indicates that the fractal nature of the network structure of PDTS does not change with temperature but that the mechanical strength of the fractal network increases with decreasing temperature.

E. Mechanical self-similarity before the gel point

As described in Sec. II, if the clusters of the fractal network grow with self-similarity during the gelation process, the mechanical self-similarity should hold as well before the gel point. Thus, we test whether the mechanical self-similarity is observed in the PDTS/PS system. Figure 7 shows the results of the superposition of $\log_{10}G'$ and $\log_{10}G''$ vs ω at 183 °C obtained at various ε before reaching gel point. In order to obtain the master curves we shifted G' and G'' at each ε by the shift factors a_v and a_h with the constraint given by Eqs. (12) and (17). Namely, we shifted $\log_{10} G'$ and $\log_{10} G''$ vs $\log_{10}\omega$ along the straight line with a slope $n=z/(k+z)=0.68$. Here p is assumed to be proportional to t and hence ε is calculated from $\varepsilon=|t-t_c|/t_c$ with $t_c=46.8$ min. In Fig. 7 a_v and a_h are, respectively, vertical and horizontal shift factors at each p, and we can obtain the master curves for G' and G'' measured at various ε before reaching gel point and observed the $\omega^{2/3}$ power law at a high frequency region. When the system is close to the gelation point, very large clusters appear and smaller clusters may be considered as the matrix. This situation is very similar to the mechanical behavior of the dilute solution of polymers. The deviation of the mechanical behavior from the $\frac{2}{3}$ power law of ω at the low frequency limit is due to the break of the self-similarity at the length scale greater than ξ and is attributed to the terminal flow behavior of the clusters as a whole.

In Figure 8, the logarithmic shift factors $\log_{10} a_v$ and $\log_{10} a_h$ are plotted as functions of $\varepsilon(p)/\varepsilon(p_r)$. Here again

TABLE I. Characteristic time for formation of the critical gel or gel point, t_c, loss tangent at t_c, tan δ, the exponent n,$n_{\tan}$, obtained from tan δ at gel point, or n_{slope}, obtained from $\log_{10} G'$ and $\log_{10} G''$ vs $\log_{10}\omega$ plot, and gel strength S at each temperature.

Temp. (°C)	t_c (min)	tan δ	$n_{\tan}$	n_{slope}	$10^{-2}S$ (Pa s^n)
183	46.8	1.84	0.68±0.02	0.68±0.02	9.93
181	29.0	1.84	0.68±0.02	0.68±0.02	19.8
178	16.7	1.63	0.65±0.02	0.65±0.02	23.0

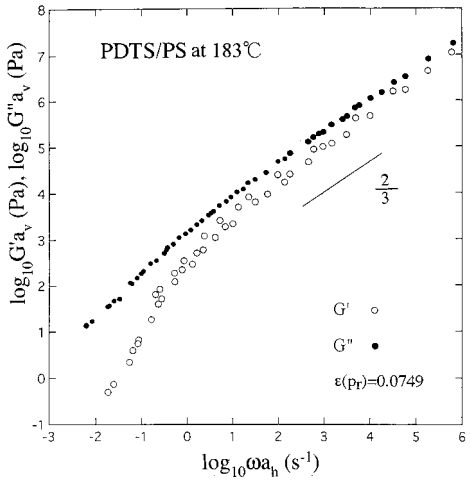

FIG. 7. Superposition of frequency dependence of G' and G'' obtained at various ε before gelation point along a straight line with a slope n at 183 °C.

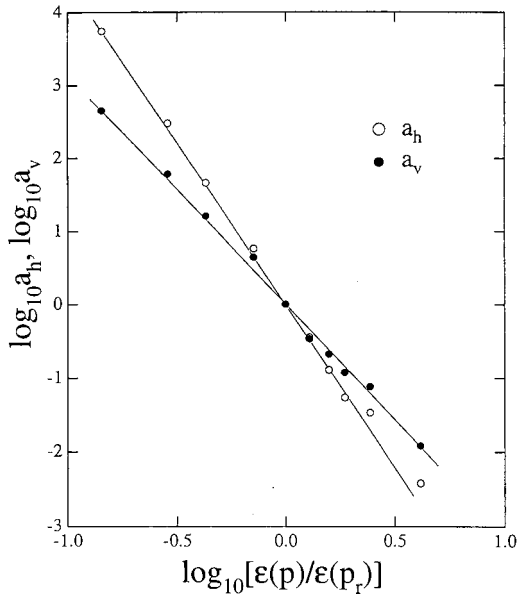

FIG. 8. Shift factors a_v and a_h are plotted against $\varepsilon/(p)/\varepsilon(p_r)$ for the gelation process of the PDTS/PS system at 183 °C.

we assume $p \propto t$. Each plot gives a straight line and the slope is $-z$ for $\log_{10} a_v$ and $-(k+z)$ for $\log_{10} a_h$. The values of k and z are 1.4 ± 0.1 and 3.1 ± 0.1, respectively. The crystallization of PDTS gives a larger value of z than the chemical gelation system such as end-linking polymers [13], indicating that the PDTS/PS system forms more dense networks than the chemical gels in which the gelation occurs by the chemical cross-linking reaction between the end points of prepolymers. On the other hand, the gelation in our system occurs by crystallization of PDTS so that the networks of PDTS systems consist of the fibrils of the crystalline structures of PDTS. The cross-linking reaction in chemical gels is restricted to the end points of prepolymers, while the physical ''cross linking'' via crystallization of PDTS can occur at any points of fibrils. Thus, the PDTS system is expected to form more dense networks than the chemical gels.

In order to check the postulate that the longest relaxation time of the gel diverges with the same critical exponent from both sides of the gel point, we have to investigate the scaling relation of J_e^0 [Eq. (4)]. However, we did not measure the frequency range low enough to determine J_e^0 so that it is difficult to check the postulate. This point should be solved in the future.

V. CONCLUSIONS

We investigated time evolution of the viscoelasticity of the physical gel of the PDTS/PS system during the sol-gel transition process. At the gel point, the power-law behavior $G' \sim G'' \sim \omega^n$ was observed. The observed n is independent of the gelation temperature T and agrees with the value $n = \frac{2}{3}$ predicted by the percolation theory without hydrodynamic interactions, although S increases with decreasing T. This observation indicates that the fractal network structure of PDTS itself does not change with T but that the mechanical strength of the fractal networks increases with decreasing T. Before reaching gel point, G' and G'' can be well superposed onto the master curves, indicating that both the structural self-similarity and mechanical self-similarity hold before reaching gel point.

ACKNOWLEDGMENTS

This work was supported in part by a Grant-in-Aid from the Japan Society for the Promotion of Science (12640392 and 12305060) and by a Grant-in-Aid from the Ministry of Education, Culture, Sports, Science, and Technology, Japan.

[1] T. Kobayashi, H. Hasegawa, and T. Hashimoto, J. Soc. Rheol., Jpn. **17**, 86 (1989).
[2] A. Shah. *Handbook of Polyvinyl Chloride Formulating* (Wiley, New York, 1993), p. 699.
[3] H. H. Winter and M. Mours, Adv. Polym. Sci. **134**, 165 (1997).
[4] F. Chambon and H. H. Winter, J. Rheol. **31**, 683 (1987).
[5] H. H. Winter, Prog. Colloid Polym. Sci. **75**, 104 (1987).
[6] H. H. Winter, P. Moraanelli, and F. Chambon, Macromolecules **21**, 532 (1988).
[7] J. C. Scanlan and H. H. Winter, Macromolecules **24**, 47 (1991).
[8] A. Izuka, H. H. Winter, and T. Hashimoto, Macromolecules **25**, 2422 (1992).
[9] D. Durand, M. Delsanti, M. Adam, and J. M. Luck, Europhys. Lett. **3**, 297 (1987).
[10] D. Adolf, J. E. Martin, and J. P. Wilcoxon, Macromolecules **23**, 527 (1990).
[11] D. F. Hodgson and E. I. Amis, Macromolecules **23**, 2512 (1990).
[12] R. Mullen, E. Gerard, P. Dugand, P. Rempp, and Y. Gnanou, Macromolecules **24**, 1321 (1991).
[13] M. Takahashi, K. Yokoyama, and T. Masuda, J. Chem. Phys.

101, 798 (1994).
[14] J. E. Martin, D. Adolf, and J. P. Wilcoxon, Phys. Rev. A **39**, 1325 (1989).
[15] M. Rubinstein, R. H. Colby, and J. R. Gillmor, Polym. Prepr. (Am. Chem. Soc. Div. Polym. Chem.) **30**, 81 (1989); in *Space-Time Organization in Macromolecular Fluids*, edited by F. Tanaka, M. Doi, and T. Ohta (Springer-Verlag, Berlin, 1989).
[16] M. Muthukumar, J. Chem. Phys. **83**, 3162 (1985).
[17] M. Muthukumar, Macromolecules **22**, 4656 (1989).
[18] W. Hess, T. A. Vilgis, and H. H. Winter, Macromolecules **21**, 2536 (1988).
[19] T. Takigawa, M. Takahashi, K. Urayama, and T. Masuda, Chem. Phys. Lett. **195**, 509 (1992).
[20] P. G. de Gennes, *Scaling Concepts in Polymer Physics* (Cornell University, Ithaca, NY, 1979).
[21] B. Denida, D. Stauffer, H. Herrmann, and J. Vannimenus, J. Phys. (France) Lett. **44**, L701 (1983); **45**, L913 (1984).
[22] P. G. de Gennes, C. R. Seances Acad. Sci., Ser. B **286**, 131 (1978).
[23] H. J. Herrmann, B. Derrida, and J. Vannimenus, Phys. Rev. B **30**, 4080 (1984).
[24] J. D. Ferry, *Viscoelastic Properties of Polymers*, 3rd ed. (Wiley, New York, 1980).
[25] T. Kobayashi, H. Yagi, S. Kitagawa, and T. Hashimoto, J. Chem. Soc. Jpn. **7**, 850 (1993).
[26] T. Kobayashi, M. Takenaka, and T. Hashimoto (unpublished).